Impact of contact overlap on transconductance and noise in organic electrochemical transistors

Anastasios G Polyravas[1], Vincenzo F Curto[1], Nathan Schaefer[2], Andrea Bonaccini Calia[2], Anton Guimera-Brunet[3,4], Jose A Garrido[2,5] and George G Malliaras[1]

[1] Electrical Engineering Division, Department of Engineering, University of Cambridge, 9 JJ Thomson Ave, Cambridge CB3 0FA, United Kingdom
[2] Catalan Institute of Nanoscience and Nanotechnology (ICN2), CSIC, Barcelona Institute of Science and Technology, Campus UAB, Bellaterra, Barcelona, Spain
[3] Institut de Microelectronica de Barcelona, IMB-CNM (CSIC), 08193, Bellaterra, Barcelona, Spain
[4] CIBER-BBN, Networking Center on Bioengineering, Biomaterials and Nanomedicine, Barcelona, Spain
[5] ICREA, Pg. Lluís Companys 23, 08010 Barcelona, Spain

E-mail: gm603@cam.ac.uk

Received xxxxxx
Accepted for publication xxxxxx
Published xxxxxx

Abstract

Organic electrochemical transistors (OECTs) from poly(3,4-ethylenedioxythiophene) doped with polystyrene sulfonate (PEDOT:PSS) are used as amplifying transducers for bioelectronics. Although the impact on performance of device geometry parameters such as channel area and thickness has been widely explored, the overlap between the semiconductor film and the source and drain contacts has not been considered. Here we vary this overlap and explore its impact on transconductance and noise. We show that increasing contact overlap does not alter the magnitude of the steady-state transconductance but it does decreases the cut-off frequency. Noise was found to be independent of contact overlap and to vary according to the charge noise model. The results show that high quality contacts can be established in PEDOT:PSS OECTs with minimal overlap.

Keywords: organic electrochemical transistors, bioelectronics, device geometry, noise

1. Introduction

Organic electrochemical transistors (OECTs) are attracting a great deal of attention for applications in electronics and bioelectronics(1). Their operation relies on the injection of ions from an electrolyte into the volume of a semiconducting polymer. Poly(3,4-ethylenedioxythiophene) doped with polystyrene sulfonate (PEDOT:PSS), a *p*-type degenerately doped semiconductor, has become the material of choice for OECTs due to its commercial availability, stability and biocompatibility(2). Small metal cations can be readily injected in this material from a variety of electrolytes under the influence of an applied gate voltage, leading to large changes in the drain current. PEDOT:PSS OECTs have been used to detect a variety of chemical and biological analytes(3), to transduce electrophysiological activity(4,5), to develop 3D tissue models (6), and also to fabricate large-area circuitry(7) and neuromorphic devices(8).

The figure-of-merit that characterises the ability of transistors to transduce a signal is the transconductance g_m, defined as the first derivative of the drain current I_d over the gate voltage V_g. OECTs have been shown to exhibit a very high transconductance, due to the volumetric changes in the conductivity of the channel (9). A great deal of work has focused on understanding how to optimise transconductance by tuning the dimensions of the channel(1,10,11) and the properties of the semiconductor(1,12). A second parameter that is important in signal transduction is the noise produced by the transistor. Flicker noise, which decreases with frequency as 1/f, has been shown to be dominant at low

frequencies in a variety of transistor technologies(13–17), including OECTs(18). Fluctuations in the hole density inside the channel are assumed to be responsible for this behaviour(18).

An important parameter that has not yet been explored in OECTs is the overlap between the polymer film and the source and drain contacts. This overlap is usually determined by the registration of the patterning technique employed to define the top layer. In thin film transistors, such design parameters are known to affect performance through changes in contact resistance and overlap capacitance(19). Here we explore how this overlap affects transconductance and noise in PEDOT:PSS OECTs.

2. Materials and methods

2.1 Device fabrication

The fabrication of OECTs was based on the parylene peel-off processes published previously(20) and included the deposition of gold, parylene C and PEDOT:PSS films. Glass slides (Knittel Glass) with dimensions of 26×76 mm^2 were used as substrates. They were cleaned by an ultrasonic bath in a dilute solution of Micro-90 (Cole Parmer) in deionised water (DI) for 20 minutes, rinsed with DI water, and sonicated again inside an acetone - isopropyl alcohol solution (90%-10%) for another 20 minutes. To pattern the metal pads a negative photoresist, AZ nLOF2035 (MicroChemicals GmbH), was spun on the glass substrate at 4000 rpm for 30 seconds, baked at 110ºC for 1 minute and exposed to UV light using a mask aligner (Karl Suss MA/BA6). The samples were then baked at 110ºC for 1 minute and developed using a MIF 726 developer. They were activated for 2 minutes using an O_2 plasma cleaner (Diener Electronic Femto) and placed inside an e-beam evaporator (Kurt J. Lesker PVD-75) for metallization. A thin layer of Ti (5nm) was deposited to aid adhesion, followed by 100 nm of gold. An overnight lift-off, using Technistrip NI555 (MicroChemicals GmbH) led to the final metal patterns.

The samples were activated again for 2 minutes and submerged in an ethanol solution of the adhesion promoter 3-(trimethoxysilyl)propyl methacrylate (Sigma Aldrich A-174) for 30 sec, then hard-baked on a hotplate at 70ºC for an hour. Subsequently, they were placed in a parylene coater (SCS) and 2 µm of parylene C was deposited. An anti-adhesive layer of Micro-90 in DI water (2% v/v soap solution) was spun at 1000 rpm, and a second (sacrificial) layer of parylene C was deposited. A layer of photoresist AZ9260 (MicroChemicals GmbH) was then spun on the samples at 4500 rpm for 30 seconds and was post baked at 110ºC for two minutes. The samples were exposed to UV light, and developed for 6 minutes using a MIF 726 developer. Reactive ion etching (Oxford 80 Plasmalab plus) opened the window for the deposition of the PEDOT:PSS. 19 ml of Clevios PH1000 (Heraeus), 1 ml of ethylene glycol, 50 µl of dodecyl benzene sulfonic acid (DBSA, Sigma Aldrich) and 0.2 ml of (3-glycidyloxypropyl)trimethoxysilane (GOPS, Sigma Aldrich) were mixed and sonicated for 15 minutes. The surface was activated and the PEDOT:PSS dispersion was spun at 3000 rpm for 30 seconds. The samples were annealed at 110ºC for 1 minute and the sacrificial layer of parylene C was peeled off. Finally, the samples were hard baked at 130ºC for an hour and immersed into DI water overnight to remove any excess compounds.

2.2 Device characterization

An optical microscope (Nikon Eclipse LV100ND) was used to verify that the target dimensions were within 2 µm of the target values. A Bruker Dimension Icon AFM was used to verify that film morphology does not change with contact overlap (Figure S1 in Supplementary Information). A Dektak XT stylus profilometer (Bruker) was used to measure the thickness of the PEDOT:PSS. Transistors were characterised using a 0.01 M Phosphate Buffered Saline (PBS) solution and a Ag/AgCl gate electrode (World Precision Instruments). Electrical measurements were performed inside a Faraday cage. A semiconductor device analyser (Keysight B1500A) was employed to measure the output and transfer curves. A delay of at least 100 ms was applied between sourcing voltage

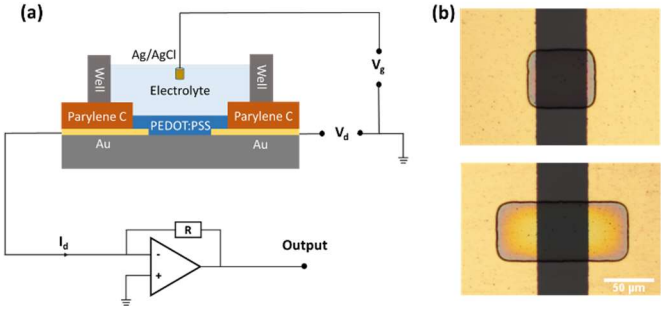

Figure 1. a) Schematic of an OECT and digram of the circuit used for the noise measurements. b) Optical micrograph of OECTs with 10% (top) and 70% (bottom) contact overlap.

and measuring current to ensure that the latter reached steady state. The frequency response of the devices was measured with two NI-PXI-4071 digital multimeters controlled by LabVIEW. The OECTs were biased at a constant V_d while the gate was biased with a series of sine waves of 50 mV amplitude and frequency between 1 Hz and 20 kHz. Noise was measured using a custom-built transimpedance amplifier with 10k gain(21), as shown in Figure 1(a). The output was split into DC (< 0.1 Hz) and AC (0.1 Hz < frequency < 5 kHz) components and the latter was amplified by an additional factor of 100 and recorded with a data acquisition system (National Instruments USB-6363). An FFT transformation was performed to calculate the power spectral density of the drain current fluctuations S_{Id}. Customised software in MATLAB removed the 50 Hz noise and its harmonics, and S_{id}

was smoothed with the smooth() function. Figures S2(a) and S2(b) in Supplementary Information show the effects of filtering and smoothing on the data.

3. Results and discussion

3.1 Contact overlap

In order to investigate the impact of contact overlap on device performance, we fabricated arrays of OECTs with a fixed source and drain electrode geometry and varied the dimensions of the PEDOT:PSS film spanning the Au contacts, as seen in Figure 1(b). The OECTs had a channel length L=50 µm (defined by the distance between the source and drain contacts), a width W=50 µm (defined by the width of the PEDOT:PSS film) and channel thickness d~100 nm (defined by the thickness of the PEDOT:PSS film). These dimensions were chosen as they lead to devices with performance that is suitable for cutaneous electrophysiology(11). The overlap between the PEDOT:PSS film and the source and drain contacts was varied to 5, 15, 25 and 35 µm respectively, leading to 10%, 30%, 50% and 70% overlap between PEDOT:PSS film and contact, respectively. Optical micrographs of OECTs with 10% and 70% contact overlap are shown in Figure 1(b). The OECTs operated in depletion mode (Figure S3 in Supplementary Information), consistent with previously published data(22).

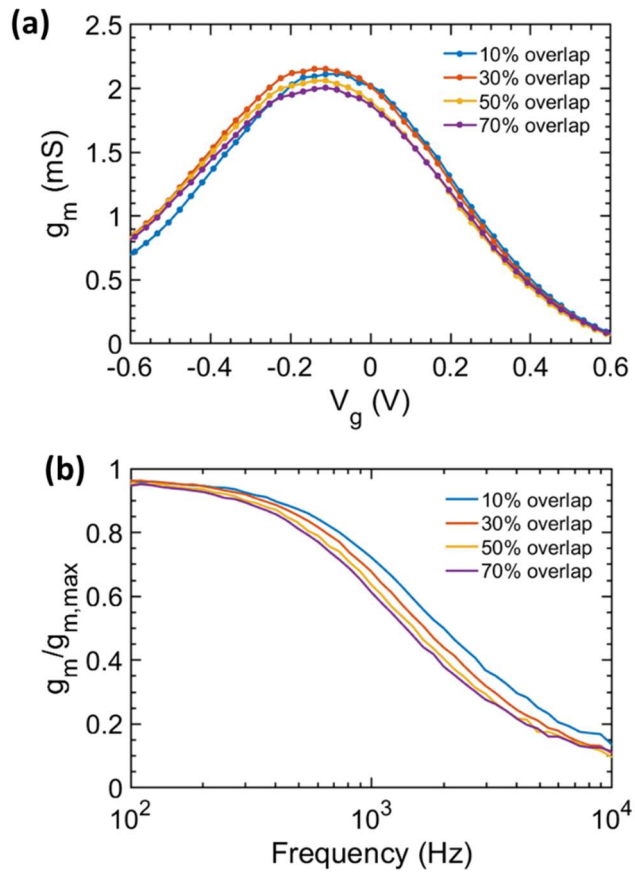

Figure 2. a) Transconductance as a function of V_g for OECTs with different contact overlap at V_d=-0.6 V. Lines are guides to the eye. b) Corresponding normalised transconductance vs. frequency.

3.2 Impact on transconductance

Figure 2(a) shows the dependence of the transconductance g_m on V_g for OECTs with different contact overlaps. These four OECTs were fabricated on the same glass slide and were equally spaced from the centre, to ensure similar PEDOT:PSS film thickness. The data shows no systematic variation in g_m as a function of contact overlap. This is not surprising, as all devices have the same nominal channel dimensions. It means that a high-quality ohmic contact is achieved at both the source and the drain, even for the OECT with the smallest overlap.

The frequency dependence of g_m for the four transistors with different contact overlaps is shown in Figure 2(b). A systematic decrease in the cut-off frequency $f_c=g_{m,max}/\sqrt{2}$ is observed as the overlap increases: The OECT with 70% contact overlap is ~300 Hz slower than the one with 10% contact overlap. The cut-off frequency of transistors depends on the RC time constant of the gate circuit(23). In OECTs, the capacitance C arises from the charging of the polymer film with ions(24). The data indicates that the capacitance that is important here is the one associated with the entire volume of the PEDOT:PSS film, rather than with just the area between the source and drain contact. At the same time, the resistance R depends on the perimeter of the PEDOT:PSS film(25). A calculation based on these arguments (see Supplementary Information) predicts a change in f_c of 287 Hz, in close agreement to the measured value.

3.3 Impact on noise

Consistent with previous measurements in electrolyte gated transistors, the power spectral density of the drain current fluctuations S_{Id} was found to follow a 1/f dependence (Figure S4 in Supplementary Information)(14,17,18). The normalised power spectral density S_{Id}/I_d^2, also referred to as the relative noise, is often used in literature to compare data from different devices and bias conditions. Figure 3(a) shows the relative noise at 10 Hz as a function of V_g, for different values of contact overlap. The value of 10 Hz was selected as it corresponds to the strongest brain rhythm (alpha wave) in encephalography(26). The data shows no systematic variation in noise as a function of contact overlap. This is consistent with the fact that device performance, as seen by the steady-state transconductance, does not vary with contact overlap. It means that the relevant feature that determines noise is the channel length and not the length of the PEDOT:PSS film.

Figure 3(b) shows that relative noise scales with g_m^2/I_d^2. This is consistent with the charge noise model(27,28), according to which the measured noise in the drain current

originates from fluctuations in the hole density inside the channel. Noise can therefore be referred to voltage fluctuations at the gate according to $S_{id} = g_m^2 \cdot S_{Vg}$, where S_{Vg} is the gate-referred noise(27,28). The line is a fit to the model

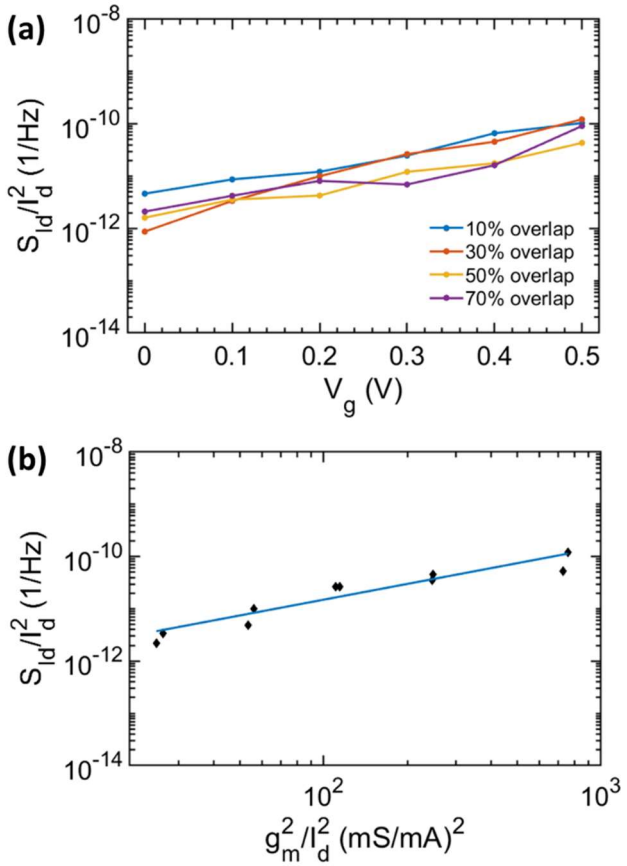

Figure 3. a) Relative noise at 10 Hz vs. V_g for OECTs with different contact overlaps at V_d=-0.5 V. Lines are guides to the eye. b) relative noise at 10 Hz vs. g_m^2/I_d^2 for OECTs with 30% contact overlap and different values of V_g and V_d=-0.5 V. The line is a fit to the charge noise model.

yielding $S_{Vg} = 12.7 \cdot 10^{-14}$ V^2/Hz. This value, corrected for channel dimensions, compares favourably to previous measurements in PEDOT:PSS OECTs(18) and electrolyte-gated graphene transistors(17). Additional characterisation data are shown in Figures S5 and S6 in Supplementary Information.

3.4 Discussion

Simple fabrication, biocompatibility and high transconductance make OECTs excellent candidates for recording of biological signals. They are particularly well suited for recording cutaneous electrophysiology(29), as these signals typically occur below 100 Hz and have low amplitudes. The latter range from mV for signals from muscles to tens of µV for brain activity recordings. According to the change noise model, the noise V_{rms} during a recording with a bandpass filter set between 1 and 100 Hz can be calculated by:

$$V_{rms} = \sqrt{\frac{\int_{1\,Hz}^{100\,Hz} S_{I_d} \cdot df}{g_m{}^2}}. \qquad (1)$$

Accordingly, we find V_{rms}= 3.4 µV. This value is more than adequate for enabling recordings of cutaneous electrophysiology with high signal-to-noise ratio (SNR) (29,30).

Previous studies showed that the trade-off between gain and bandwidth can be navigated in OECTs by adjusting channel thickness: Increasing channel thickness increases transconductance but decreases the cut-off frequency(11). An additional design rule identified here calls for minimizing contact overlap, as the latter only serves to make the OECT slower and does not affect steady-state transconductance and noise.

4. Conclusions

In this work, we investigated how overlap between the PEDOT:PSS film and the source and drain contacts affects OECT performance. We find that while steady-state transconductance and noise remain the same, the cut-off frequency decreases with increasing contact overlap. This calls for minimising this overlap to achieve the best performing devices.

Acknowledgements

This work was funded by the European Union's Horizon 2020 research and innovation programme under grant agreement no. 732032 (BrainCom). We thank Ioannis Prattis (CGC) for the fruitful discussions and the assistance he provided with the AFM measurements.

References

1. Rivnay J, Inal S, Salleo A, Owens RM, Berggren M, Malliaras GG. Organic electrochemical transistors. Nature Reviews Materials. 2018 Feb;3(2):17086.

2. Mantione D, del Agua I, Sanchez-Sanchez A, Mecerreyes D, Mantione D, del Agua I, et al. Poly(3,4-ethylenedioxythiophene) (PEDOT) Derivatives: Innovative Conductive Polymers for Bioelectronics. Polymers. 2017 Aug 11;9(8):354.

3. Lin P, Yan F. Organic Thin-Film Transistors for Chemical and Biological Sensing. Advanced Materials. 2012 Jan 3;24(1):34–51.

4. Khodagholy D, Doublet T, Quilichini P, Gurfinkel M, Leleux P, Ghestem A, et al. *In vivo* recordings of brain activity using organic transistors. Nature Communications. 2013 Mar 12;4:1575.

5. Campana A, Cramer T, Simon DT, Berggren M, Biscarini F. Electrocardiographic Recording with Conformable Organic Electrochemical Transistor Fabricated on Resorbable Bioscaffold. Advanced Materials. 2014;26(23):3874–8.

6. Pitsalidis C, Ferro MP, Iandolo D, Tzounis L, Inal S, Owens RM. Transistor in a tube: A route to three-dimensional bioelectronics. Science Advances. 2018 Oct 1;4(10):eaat4253.

7. Sun H, Vagin M, Wang S, Crispin X, Forchheimer R, Berggren M, et al. Complementary Logic Circuits Based on High-Performance n-Type Organic Electrochemical Transistors. Advanced Materials. 2018;30(9):1704916.

8. Burgt Y van de, Melianas A, Keene ST, Malliaras G, Salleo A. Organic electronics for neuromorphic computing. Nature Electronics. 2018 Jul;1(7):386.

9. Khodagholy D, Rivnay J, Sessolo M, Gurfinkel M, Leleux P, Jimison LH, et al. High transconductance organic electrochemical transistors. Nature Communications. 2013 Jul 12;4:2133.

10. Rivnay J, Leleux P, Sessolo M, Khodagholy D, Hervé T, Fiocchi M, et al. Organic Electrochemical Transistors with Maximum Transconductance at Zero Gate Bias. Adv Mater. 2013 Dec 1;25(48):7010–4.

11. Rivnay J, Leleux P, Ferro M, Sessolo M, Williamson A, Koutsouras DA, et al. High-performance transistors for bioelectronics through tuning of channel thickness. Science Advances. 2015 May 1;1(4):e1400251.

12. Inal S, Malliaras GG, Rivnay J. Benchmarking organic mixed conductors for transistors. Nature Communications. 2017 Nov 24;8(1):1767.

13. Klaassen FM. Characterization of low 1/f noise in MOS transistors. IEEE Transactions on Electron Devices. 1971 Oct;18(10):887–91.

14. Sharf T, Kevek JW, DeBorde T, Wardini JL, Minot ED. Origins of Charge Noise in Carbon Nanotube Field-Effect Transistor Biosensors. Nano Lett. 2012 Dec 12;12(12):6380–4.

15. Clément N, Nishiguchi K, Dufreche JF, Guerin D, Fujiwara A, Vuillaume D. A silicon nanowire ion-sensitive field-effect transistor with elementary charge sensitivity. Appl Phys Lett. 2011 Jan 3;98(1):014104.

16. Rhayem J, Rigaud D, Valenza M, Szydlo N, Lebrun H. 1/f Noise in amorphous silicon thin film transistors: effect of scaling down. Solid-State Electronics. 1999 Apr 1;43(4):713–21.

17. Heller I, Chatoor S, Männik J, Zevenbergen MAG, Oostinga JB, Morpurgo AF, et al. Charge Noise in Graphene Transistors. Nano Lett. 2010 May 12;10(5):1563–7.

18. Stoop RL, Thodkar K, Sessolo M, Bolink HJ, Schönenberger C, Calame M. Charge Noise in Organic Electrochemical Transistors. Phys Rev Applied. 2017 Jan 12;7(1):014009.

19. Münzenrieder N, Salvatore GA, Petti L, Zysset C, Büthe L, Vogt C, et al. Contact resistance and overlapping capacitance in flexible sub-micron long oxide thin-film transistors for above 100 MHz operation. Appl Phys Lett. 2014 Dec 29;105(26):263504.

20. Sessolo M, Khodagholy D, Rivnay J, Maddalena F, Gleyzes M, Steidl E, et al. Easy-to-Fabricate Conducting Polymer Microelectrode Arrays. Adv Mater. 2013 Apr 18;25(15):2135–9.

21. Hébert C, Masvidal-Codina E, Suarez-Perez A, Calia AB, Piret G, Garcia-Cortadella R, et al. Flexible Graphene Solution-Gated Field-Effect Transistors: Efficient Transducers for Micro-Electrocorticography. Advanced Functional Materials. 2018;28(12):1703976.

22. Bernards DA, Malliaras GG. Steady-State and Transient Behavior of Organic Electrochemical Transistors. Adv Funct Mater. 2007 Nov 23;17(17):3538–44.

23. Sze SM, Ng KK. Physics of Semiconductor Devices. 3rd edition. Hoboken, N.J: Wiley-Blackwell; 2006. 832 p.

24. Proctor CM, Rivnay J, Malliaras GG. Understanding volumetric capacitance in conducting polymers. Journal of Polymer Science Part B: Polymer Physics. 2016 Aug 1;54(15):1433–6.

25. Koutsouras DA, Gkoupidenis P, Stolz C, Subramanian V, Malliaras GG, Martin DC. Impedance Spectroscopy of Spin-Cast and Electrochemically Deposited PEDOT:PSS Films on Microfabricated Electrodes with Various Areas. ChemElectroChem. 2017;4(9):2321–7.

26. Buzsaki G. Rhythms of the Brain. 1 edition. Oxford ; New York: Oxford University Press, U.S.A.; 2011. 464 p.

27. Tersoff J. Low-Frequency Noise in Nanoscale Ballistic Transistors. Nano Lett. 2007 Jan 1;7(1):194–8.

28. Bedner K, Guzenko VA, Tarasov A, Wipf M, Stoop RL, Rigante S, et al. Investigation of the dominant 1/f noise source in silicon nanowire sensors. Sensors and Actuators B: Chemical. 2014 Feb 1;191:270–5.

29. Leleux P, Rivnay J, Lonjaret T, Badier J-M, Bénar C, Hervé T, et al. Organic Electrochemical Transistors for Clinical Applications. Advanced Healthcare Materials. 2015;4(1):142–7.

30. Thakor NV. Translating the Brain-Machine Interface. Science Translational Medicine. 2013 Nov 6;5(210):210ps17-210ps17.